

## Sounder Design Considerations in the Selection of Temperature Sensing Channels

MILTON HALEM AND MING-DAH CHOW<sup>1</sup>

*Institute for Space Studies, Goddard Space Flight Center, NASA, New York, N. Y. 10025*

(Manuscript received 4 March 1975, in revised form 8 January 1976)

### ABSTRACT

Simulation studies on the performance of IR sounders under varying conditions of cloud cover and cloud heights are carried out for Nimbus 6. An analytic function is derived for calculating the relative response to cloud height errors for arbitrary cloud-sensing channels. Based on the values of the response function, the best choice of channels for determining cloud amounts are obtained. An algorithm is described for determining cloud heights and the sensitivity of cloud-height sensing channels are tested. It is found that for the HIRS instrument, the most transparent channel in the 4.3  $\mu\text{m}$  band is optimal for adjusting cloud heights while the channel in the 15  $\mu\text{m}$  band peaking closest to the surface is best for determining cloud amounts.

### 1. Introduction

A principal consideration in the design of satellite temperature sounders is the choice of sensing channels. Previous studies leading to the selection of channels concentrated on choosing frequency bands with sharp, well-separated weighting functions to yield improved vertical resolution. This consideration finally led to meteorological satellites such as Nimbus 6 carrying a family of sounders with different spectral ranges. However, overlooked in this development was the need to consider overall system performance, where the response to atmospheric effects such as clouds varies with the individual channels.

Experience with the VTPR instrument on NOAA 2 has shown that the presence of clouds in the radiometer field of view is the chief factor influencing the accuracy and yield of sounding temperature profiles. The difficulty in accounting for clouds in the numerical derivation of temperature profiles stems from the uncertainties in determining cloud heights, cloud amounts and their optical properties. The response in the different channels to errors introduced through the determination of these cloud parameters in large part accounts for the wide fluctuations in the accuracy of the derived temperature profiles. A proper selection of channel frequencies in the shortwave IR, longwave IR, and microwave regions can provide the numerical analyst with alternate schemes to minimize the effects of clouds, thereby increasing the accuracy and yield.

Studies at GISS, with actual VTPR data, show that using fixed cloud heights based on climatology

and varying as a function of latitude provide globally averaged temperature accuracies comparable to methods which compute cloud heights and offer considerable savings in computer time. Errors arising from inaccurate determinations of cloud heights are compensated to some extent by adjustments in the calculated cloud cover. Although average rms temperature errors are comparable, theoretically, it should be possible to improve the overall temperature accuracy by improving the instrument's performance in regions of heavy cloud cover. Sounders with channels in widely separated bands such as for Nimbus 6 provide redundant information which can be useful in determining cloud heights and cloud amount, i.e., algorithms can be derived which take advantage of channels peaking at same pressure levels in different IR regions.

To test the advantages that might be gained from such a system, simulation studies have been carried out for the Nimbus 6 sounders, under varying conditions of cloud cover and cloud heights. Results indicate that sounding temperature accuracies are sensitive to cloud height errors only in regions with high (above 500 mb) clouds and heavy (more than 50%) cloud cover, and are relatively insensitive in regions with moderately low clouds (below 500 mb) and light (less than 50%) cloud cover.

Further analysis of the sensitivity of the calculations of outgoing radiance to variations in cloud height errors show large differences for different channels. An analytic expression has been derived for calculating this response which provides a useful estimate for determining the temperature errors at the different pressure levels as a function of cloud height errors. Calculations of the relative response function for the Nimbus 6 channels are presented in Section 3.

<sup>1</sup> NAS-NRC Research Associate.

An algorithm for determining cloud heights based on a single field of view is described in Section 4. Simulation studies using this algorithm under conditions of high clouds and heavy cloud cover yield temperatures with accuracies comparable to that obtained under clear conditions. This method differs from Chahine's (1974) approach where he finds that the best channels to use for cloud sounding frequencies on multispectral sounders are in the 15  $\mu\text{m}$  band. We also find the 15  $\mu\text{m}$  band best for determining cloud amounts but, in our method, the 4.3  $\mu\text{m}$  band is best for adjusting cloud heights. This difference may stem from the fact that our methods assume surface temperatures available from other observations while Chahine solves for the surface temperatures as well as cloud parameters.

## 2. Derivation of temperature profiles

Meteorological satellites measure the outgoing radiances in several spectral channels in the 4.3  $\mu\text{m}$ , 15  $\mu\text{m}$  and microwave regions of the  $\text{CO}_2$  and  $\text{O}_2$  bands. Atmospheric temperature profiles are derived from these measurements by solving a set of integral radiative transfer equations. The governing radiative transfer equations for a nonscattering atmosphere in local thermodynamic equilibrium are assumed to apply over a field of view which is partly covered by a single-layer cloud at pressure  $p_c$  with cloud fraction  $N$ . The computed vertical outgoing radiances  $I(\nu_i)$  at wavenumbers  $\nu_i$ ,  $i=1, 2, \dots, K$ , are expressed as

$$I(\nu_i) = (1-N)I_{\text{clr}}(\nu_i) + NI_{\text{cld}}(\nu_i), \quad (1)$$

where  $I_{\text{clr}}$  and  $I_{\text{cld}}$  denote the outgoing radiances that would be calculated if the fields of view were completely clear or cloudy respectively; they are given by

$$I_{\text{clr}}(\nu_i) = B(\nu_i, p_s) \tau(\nu_i, p_s) + \int_{\tau(\nu_i, p_s)}^1 B(\nu_i, p) d\tau(\nu_i, p), \quad (2)$$

$$I_{\text{cld}}(\nu_i) = B(\nu_i, p_c) \tau(\nu_i, p_c) + \int_{\tau(\nu_i, p_c)}^1 B(\nu_i, p) d\tau(\nu_i, p). \quad (3)$$

In Eqs. (1)–(3) the earth's surface and cloud top are assumed to behave as blackbodies,  $p_s$  and  $p_c$  denote surface and cloud-top pressures, respectively,  $B[\nu_i, T(p)]$  is the Planck radiance, and  $\tau(\nu_i, p)$  is the atmospheric transmission function between satellite sensors and the pressure level  $p$ .

The current method used at GISS for deriving temperature profiles employs a shape-preserving iterative technique developed by Chahine (1974) for the solution of Eq. (1). The outgoing radiances  $I^j(\nu_i)$  at the  $j$ th iteration are calculated from (1) using fixed values of  $p_c$ ,  $N$  and  $T^j(p)$ . The temperatures at the next iteration  $T^{j+1}(p)$  are computed for the pressure levels where the "Planck-modified weighting functions,"

$B[\nu_i, T(p)] \partial \tau(\nu_i, p) / \partial \ln p$ , have their peaks. At any of these pressure levels, we obtain a value of Planck radiance for the next iteration  $j+1$  as

$$B^{j+1}(\nu_i, p_i) = B^j(\nu_i, p_i) \bar{I}(\nu_i) / I^j(\nu_i), \quad i=1, 2, \dots, K, \quad (4)$$

where  $\bar{I}(\nu_i)$  is the satellite-measured radiance,  $K$  the number of spectral channels, and  $p_i$  the pressure level where the curve  $B[\nu_i, T(p)] \partial \tau(\nu_i, p) / \partial \ln p$  has its maximum. At the maximum of each channel, a temperature  $T^{j+1}(p_i)$  is computed from  $B^{j+1}(\nu_i, T)$ . The temperatures at the pressure levels other than  $p_i$  are computed from

$$T^{j+1}(p) = \alpha^j(p) T^j(p), \quad (5)$$

and the value of  $\alpha^j(p)$  is linearly interpolated in  $\ln p$  between values of  $\alpha^j(p_i)$  where

$$\alpha^j(p_i) = T^{j+1}(p_i) / T^j(p_i). \quad (6)$$

If the convergence criterion is not satisfied within five iterations a slower iteration scheme which smooths out random noise is then used. Temperatures at each of the pressure levels  $p_i$  are computed using the weights

$$T^{j+1}(p_i) = T^j(p_i) \sum_{k=1}^K \alpha^j(p_k) W^j(p_k) / \sum_{k=1}^K W^j(p_k), \quad (7)$$

where

$$W^j(p_k) = \frac{B^j(p_k) \partial \tau(\nu_k, p_k)}{I^j(\nu_k) \partial \ln p}. \quad (8)$$

In calculating  $I(\nu_i)$  from Eq. (1), the cloud heights are required as specified input. In the current version, cloud heights are specified from climatological distributions according to latitudinal belts. Once the values of  $p_c$  and  $T^j(p)$  are given, a set of temperature profiles  $T^{j+1}(p, N)$  can be obtained as a function of the cloud amount  $N$ .

The cloud amount is determined by first assuming three fixed values (0, 0.50 and 0.95) of the cloud amount parameter and solving for the temperature profile in each case. The cloud amount is obtained by interpolating the derived surface temperatures to match a specified observed surface temperature from an independent observation (Jastrow and Halem, 1973).

## 3. Temperature response to cloud height errors

When cloud height errors are introduced in the derivation of temperature profiles, their effects are propagated into the calculation of the outgoing radiances. The resultant calculation of cloud amount partially compensates for the error in the calculated outgoing radiance. For example, if the clouds are assumed too high, the calculated cloud amount is smaller than it should be. This compensation in cloud amount brings about a change in the shape of the

derived temperature profiles which is directly related to the temperature error. An analytic expression is derived below which estimates the accuracies of the sounding temperature as a function of cloud height errors.

Assuming an exact knowledge of the vertical temperature profile as available from radiosonde observations and an exact knowledge of the atmospheric transmission functions, the error in the radiance for any channel produced by small uncertainties in cloud height and cloud amount can be calculated from a Taylor series approximation of Eq. (1) as follows:

$$I[\nu, p_c, N, \bar{T}(p)] = \bar{I}(\nu) + \bar{N} \Delta p_c \left. \frac{\partial I_{\text{eld}}}{\partial p_c} \right|_{\bar{p}_c} + \Delta N [\bar{I}_{\text{eld}}(\nu) - \bar{I}_{\text{clr}}(\nu)], \quad (9)$$

where the bar quantities are the assumed known values, and

$$\bar{I}(\nu) = I[\nu, \bar{p}_c, \bar{N}, \bar{T}(p)],$$

$$\bar{I}_{\text{clr}}(\nu) = I_{\text{clr}}[\nu, \bar{T}(p)],$$

$$\bar{I}_{\text{eld}}(\nu) = I_{\text{eld}}[\nu, \bar{p}_c, \bar{T}(p)],$$

$$\Delta p_c = p_c - \bar{p}_c,$$

$$\Delta N = N - \bar{N}.$$

Prescribing an arbitrary height error  $\Delta p_c$  in Eq. (9), and solving for the associated cloud amount  $\Delta N$  in a given channel, say  $\nu_0$ , to make the calculated value  $I(\nu_0, p_c, N, \bar{T})$  agree with the measured value  $\bar{I}(\nu_0)$  yields

$$\Delta N = \bar{N} \Delta p_c \left. \frac{\partial I_{\text{eld}}}{\partial p_c} \right|_{\bar{p}_c} / [\bar{I}_{\text{clr}}(\nu_0) - \bar{I}_{\text{eld}}(\nu_0)]. \quad (10)$$

However, the calculated value of  $I[\nu, p_c, N, \bar{T}(p)]$  using these values of cloud amount and cloud height will not, in general, be equal to  $\bar{I}(\nu)$  for other channels.

The magnitude of the difference between the measured and the calculated radiance in any channel  $\nu$  obtained by substituting this value of  $\Delta N$  into Eq. (9) is

$$\Delta I(\nu) = \bar{N} \Delta p_c R(\nu_0, \nu, \bar{p}_c), \quad (11)$$

where  $\Delta I(\nu) = I[\nu, p_c, N, \bar{T}(p)] - \bar{I}(\nu)$  and the function  $R$  of cloud height for any channel  $\nu$  relative to the specified channel  $\nu_0$  is given by

$$R(\nu_0, \nu, \bar{p}_c) = \frac{\partial I_{\text{eld}}(\nu)}{\partial p_c} \bigg|_{\bar{p}_c} \frac{[\bar{I}_{\text{clr}}(\nu) - \bar{I}_{\text{eld}}(\nu)]}{[\bar{I}_{\text{clr}}(\nu_0) - \bar{I}_{\text{eld}}(\nu_0)]} \times \frac{\partial I_{\text{eld}}(\nu_0)}{\partial p_c} \bigg|_{\bar{p}_c}. \quad (12)$$

The value of  $R$  depends on the two terms in Eq. (12); the first term accounts for the direct effects of cloud height errors in a given channel, while the second

term accounts for the relative effect produced by errors in cloud cover.

This error  $\Delta I(\nu)$  in the calculated radiance provides information on the related error occurring in the derivation of the temperature profile. Since the exact solution,  $\bar{T}(p)$ , does not satisfy the measured radiances with these values of  $\Delta p_c$  and  $\Delta N$ , the temperature profile is modified in such a way as to make  $I[\nu, p_c, N, T(p)] = \bar{I}(\nu)$ . The magnitude of the modification  $\Delta T(p)$  is a measure of the error produced by these cloud parameters.

#### a. Properties of the response function $R(\nu_0, \nu, \bar{p}_c)$

One usually selects the most transparent channels for  $\nu_0$ , in calculating the relative response function  $R(\nu_0, \nu, \bar{p}_c)$ , because they are most sensitive to cloud height errors and produce the largest errors in  $\Delta I(\nu)$ . The values of  $R(\nu_0, \nu, \bar{p}_c)/\bar{I}_{\text{clr}}(\nu)$  are shown in Fig. 1 for three choices of frequency  $\nu_0$  and for a range of values of  $\bar{p}_c$ . The spectral channels used for the response function in Fig. 1 are listed in Table 1. The channels and associated noise levels are taken from the prototype HIRS instrument for Nimbus 6 (W. Smith, NESS, private correspondence). The peaks of the Planck-modified weighting function  $B[\nu, T(p)] \times \partial \tau(\nu, p)/\partial \ln p$  determine the portions of the atmosphere where their contributions to the measured radiances are substantial. The temperature profile  $\bar{T}(p)$  used for computing the values of  $R(\nu_0, \nu, \bar{p}_c)/\bar{I}_{\text{clr}}(\nu)$  is typical of the April, mid-latitude regions. Properties of  $R(\nu_0, \nu, \bar{p}_c)$  are similar when standard tropical temperatures are used.

In Table 1, the channels  $\nu = 749, 2210$  and  $2190 \text{ cm}^{-1}$  are used for determining cloud heights and cloud amounts, and the other channels are used for calculating the temperature profile. It can be seen from Fig. 1 that the values of  $R(\nu_0, \nu, \bar{p}_c)$  are positive for the temperature sensing channels listed in Table 1, except at high altitude for the  $2240 \text{ cm}^{-1}$  channel in Fig. 1a with  $\nu_0 = 749 \text{ cm}^{-1}$ . A similar calculation of  $R(\nu_0, \nu, \bar{p}_c)$  for the VTPR instrument indicated that  $R$  is always positive. Thus, the error produced in the calculated radiance will be consistently larger or smaller than the observed radiance depending on whether  $\Delta p_c$  is positive or negative, respectively.

Generally, the magnitude of  $R(\nu_0, \nu, \bar{p}_c)/\bar{I}_{\text{clr}}(\nu)$  decreases with increasing value of  $\bar{p}_c$ . For example, the value of  $R(\nu_0, \nu, \bar{p}_c)/\bar{I}_{\text{clr}}(\nu)$  decreased from  $11.2 \times 10^{-4}$  to  $2 \times 10^{-4}$  for  $\nu_0 = 2190 \text{ cm}^{-1}$  and  $\nu = 733 \text{ cm}^{-1}$  as  $\bar{p}_c$  increases from 320 to 600 mb. Furthermore, the value of  $R(\nu_0, \nu, \bar{p}_c)/\bar{I}_{\text{clr}}(\nu)$  indicates the magnitude and direction of the adjusted temperature profiles. For a case where we take  $\nu_0 = 2190 \text{ cm}^{-1}$ ,  $\bar{p}_c = 600 \text{ mb}$ , and an error in cloud height of 100 mb, the cloud parameters  $p_c$  and  $N$  that satisfy  $\bar{I}(\nu_0)$  introduce errors of 2% and 5% in the calculated radiances  $I(\nu)$  for  $\nu$  equal to 733 and  $2240 \text{ cm}^{-1}$ , respectively. In order

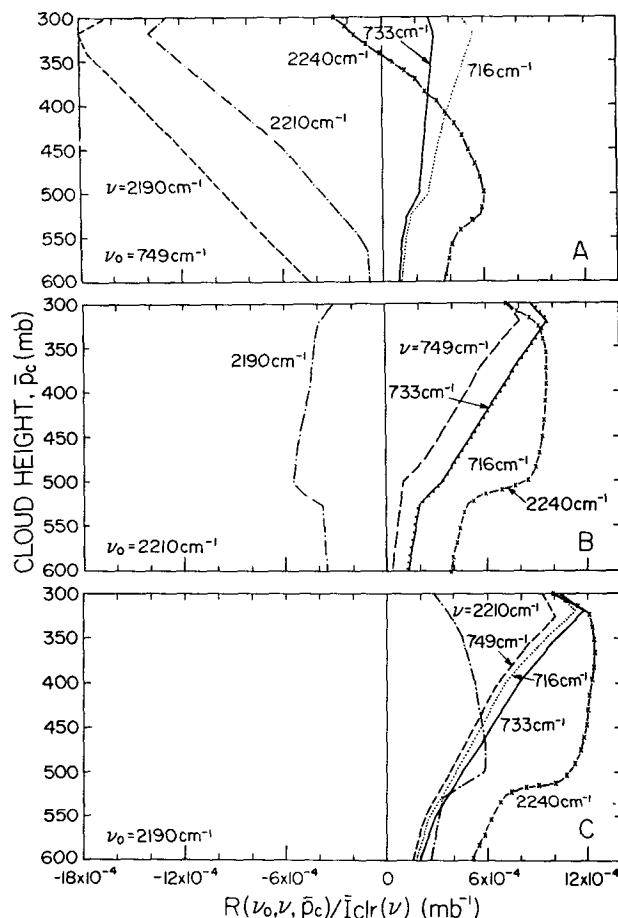


FIG. 1. Normalized radiance response function,  $R(\nu_0, \nu, \bar{p}_c) / \bar{I}_{cl}(\nu)$ , per unit cloud height error for three choices of cloud amount sensing channels,  $\nu_0 = 749, 2210$  and  $2190 \text{ cm}^{-1}$ . Radiance errors in the temperature sensing channels are seen to be smallest in Fig. 1a where  $\nu_0 = 749 \text{ cm}^{-1}$  is used to determine cloud amounts and largest in Fig. 1c for  $\nu_0 = 2190 \text{ cm}^{-1}$ .

to compensate for these errors, the correct temperatures at 800 and 625 mb are shifted to lower temperatures.

A direct estimate of the temperature errors arising from specified cloud height errors can now be derived. Let  $T(p)$  be the derived temperature profile such that  $I[\nu_i, p_c, N, T(p)] = \bar{I}(\nu_i)$ . Substituting this value of  $I[\nu_i, p_c, N, T(p)]$  into Eq. (11) and dividing by  $I[\nu_i, p_c, N, \bar{T}(p)]$ , and again applying Eq. (1) to the right-hand denominator, gives

$$1 - \frac{I[\nu_i, \bar{p}_c + \Delta p_c, \bar{N} + \Delta N, T(p)]}{I[\nu_i, \bar{p}_c + \Delta p_c, \bar{N} + \Delta N, \bar{T}(p)]} = \frac{\bar{N} \Delta p_c R(\nu_0, \nu_i, \bar{p}_c)}{\bar{I}(\nu_i) + \bar{N} \Delta p_c R(\nu_0, \nu_i, \bar{p}_c)}. \quad (13)$$

Let  $B_i / \bar{B}_i$  approximate the ratio of the outgoing radiances on the left-hand side of Eq. (13), where

$B_i$  and  $\bar{B}_i$  are the abbreviated versions of  $B[\nu_i, T(p_i)]$  and  $B[\nu_i, \bar{T}(p_i)]$  respectively. After substituting this ratio in Eq. (13), and expanding the right-hand side about  $\bar{N} \Delta p_c R / \bar{I}(\nu_i)$  which is  $\ll 1$ , we obtain

$$B_i - \bar{B}_i \approx -\bar{B}_i \frac{\bar{N} \Delta p_c R(\nu_0, \nu_i, \bar{p}_c)}{\bar{I}(\nu_i)}. \quad (14)$$

Taking a first-order approximation for  $\Delta B_i$ , one finally arrives at the direct estimate of the temperature error

$$T(p_i) - \bar{T}(p_i) \approx -\bar{B}_i \frac{\bar{N} \Delta p_c R(\nu_0, \nu_i, \bar{p}_c)}{\bar{I}(\nu_i)} \frac{\partial T}{\partial B_i} \bigg|_{B_i = \bar{B}_i}. \quad (15)$$

Eq. (15) provides an estimate of the sign and the magnitude of the temperature error as a function of the cloud height error. If the cloud height is prescribed at a lower altitude than the true cloud height (i.e.,  $\Delta p_c > 0$ ) and  $R(\nu_0, \nu, \bar{p}_c)$  is positive, then clearly the estimated temperature  $T_i$  will be colder [i.e.,  $T(p_i) < \bar{T}(p_i)$ ].

The magnitude of the temperature error depends mainly on the magnitude of the frequency response function  $R(\nu_0, \nu, \bar{p}_c)$ . Fig. 2 shows the temperature error per unit cloud height error for a situation with 50% cloud cover. Cases A, B, C consider the temperature errors for three possible channels used to determine cloud amounts. It can be seen that the magnitude of the temperature error is smaller for larger values of  $\bar{p}_c$ . It is smaller than  $0.008^\circ \text{C mb}^{-1}$  for  $\bar{p}_c > 600 \text{ mb}$  for all three cases. This means that for an error of 100 mb in the cloud heights, the errors in the derived temperatures will be less than  $0.8^\circ \text{C}$  for any pressure level. On the other hand, if  $\bar{p}_c = 400 \text{ mb}$ ,  $\bar{N} = 0.5$  and  $\Delta p_c = 100 \text{ mb}$ , errors in the derived temperatures at some pressure level could be as large as

TABLE 1. Some Nimbus 6 spectral channels and prototype instrument noise levels.

	Wavenumber ( $\text{cm}^{-1}$ )	Peak of $B(\nu, T)$ $\times \partial \tau(\nu, p) /$ $\partial \ln p$ (mb)	Instrument noise ( $\text{erg cm}^{-2}$ $\text{s}^{-1} \text{sr}^{-1} \text{cm}$ )
		$T(p)$ Stand- ard mid- latitude profile	
Temperature-sensing channels	668.5	7	2.71
	680	50	0.59
	690	120	0.45
	703	380	0.35
	2270	450	0.005
	716	575	0.40
	2240	625	0.005
Cloud-sensing channels	733	800	0.41
	749	sfc	0.31
	2210	sfc	0.005
	2190	sfc	0.005

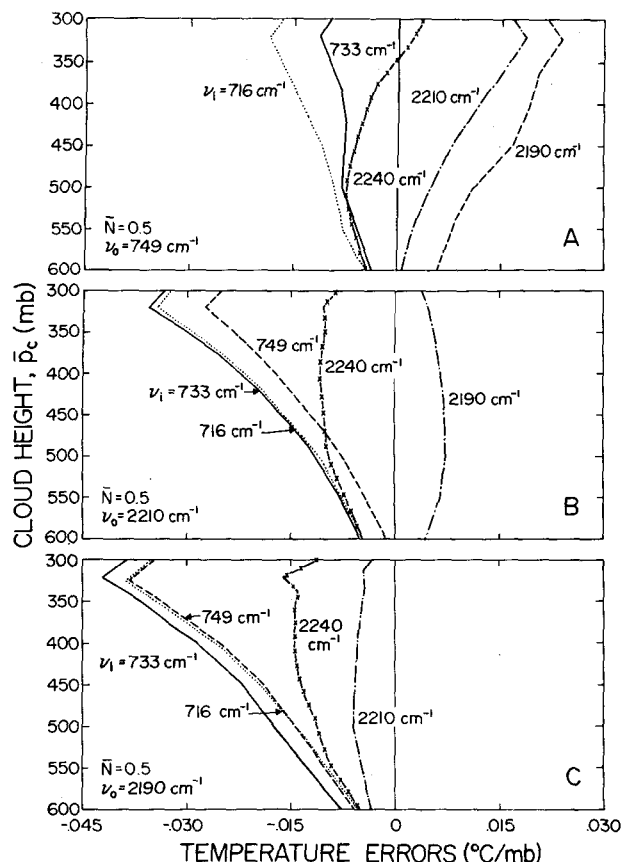


FIG. 2. Magnitude and direction of temperature errors per unit cloud height error for three choices of cloud-sensing channels. The temperature errors are largest for Fig. 2c where a 100 mb error would produce a  $-2.5^{\circ}\text{C}$  error at 575 mb, a  $-1.4^{\circ}\text{C}$  error at 625 mb and a  $-3.0^{\circ}\text{C}$  error at 800 mb, when the exact cloud height  $\bar{p}_c = 400$  mb.

$3^{\circ}\text{C}$  because of errors in cloud heights. Therefore, in regions with high clouds, errors introduced by cloud height uncertainties account for the large errors. However, by choosing the  $749\text{ cm}^{-1}$  channel for determining the cloud amounts, the effects of the cloud height errors on the derived temperature profile are smaller than they would be using the  $2210$  and the  $2190\text{ cm}^{-1}$  channels.

#### 4. A new algorithm for cloud height determinations

In the earlier work (Jastrow and Halem, 1973) an algorithm for determining the cloud height using minimum and maximum radiance measurements over a  $4^{\circ}\times 5^{\circ}$  region was described. Subsequent tests using real VTPR data showed that no significant improvements with this method are gained compared with using climatological cloud heights. The reason is that the VTPR channels are not sensitive enough to discriminate small cloud height errors. In the inversion technique described in Section 2, cloud amounts and temperature profiles are determined from specified

cloud heights and known surface temperatures. The specified cloud height  $p_c$ , the computed cloud amount  $N$ , and temperature profile  $T(p)$  satisfy the measured radiances in all of the channels used in deriving the temperature profiles.

However, the solution will not necessarily satisfy the observed radiances in the additional transparent channel in the  $4.3$  and  $15\text{ }\mu\text{m}$  regions available on the HIRS instrument. But the useful information provided by these channels make possible an automatic cloud height algorithm not possible with the VTPR. Properties of the response function  $R(\nu_0, \nu, \bar{p})$  indicate which channels should be chosen to adjust the cloud heights so as to minimize the radiance errors on the temperature sensing channels with a minimum distortion of the exact temperature profile.

If we define

$$R'(\nu_0, \nu_i, \bar{p}_c, \bar{N}) \equiv [-\bar{B}_i \bar{N} R(\nu_0, \nu_i, \bar{p}_c) / \bar{I}(\nu_i)] \partial T / \partial B_i |_{B_i = \bar{B}_i}, \quad (16)$$

then the principle idea in optimizing the instrument performance should be to select a pair of spectral channels  $(\nu_0, \nu_c)$  such that for the temperature sensing profiles  $\nu_i$  the values of  $R'(\nu_0, \nu_i, \bar{p}_c, \bar{N})$  are minimized while the difference between  $R'(\nu_0, \nu_i, \bar{p}_c, \bar{N})$  and  $R'(\nu_0, \nu_c, \bar{p}_c, \bar{N})$  is maximized. The temperature profiles derived from the set of spectral channels with small values of  $R'(\nu_0, \nu_i, \bar{p}_c, \bar{N})$  will be less sensitive to cloud height errors than those derived from the spectral channels with larger values of  $R'(\nu_0, \nu_i, \bar{p}_c, \bar{N})$ . The choice of a spectral channel  $\nu_c$  which maximizes the difference between  $R'(\nu_0, \nu_c, \bar{p}_c, \bar{N})$  and  $R'(\nu_0, \nu_i, \bar{p}_c, \bar{N})$  will make the cloud height errors easier to detect since the difference between the calculated radiance  $I[\nu_c, \bar{p}_c + \Delta p_c, \bar{N} + \Delta N, \bar{T}(p)]$  and the "measured" radiance  $\bar{I}(\nu_c)$  will also be large. In particular, the best set of spectral channels to use for Nimbus 6 are the channels with  $\nu_0 = 749\text{ cm}^{-1}$  and  $\nu_c = 2190\text{ cm}^{-1}$ .

According to the results shown in Fig. 2a with  $\nu_0 = 749\text{ cm}^{-1}$  and  $\nu_c = 2190\text{ cm}^{-1}$ , the values of  $R'(\nu_0, \nu_c, \bar{p}_c, \bar{N})$  are positive and those of  $R'(\nu_0, \nu_i, \bar{p}_c, \bar{N})$  are negative except for  $\nu_i = 2240\text{ cm}^{-1}$  at  $\bar{p}_c < 340$  mb. Negative values of  $R'(\nu_0, \nu_i, \bar{p}_c, \bar{N})$  imply that if  $p_c > \bar{p}_c$  the calculated temperature profiles will be distorted to the lower temperature side, or in general,  $T(p) < \bar{T}(p)$ . Positive values of  $R'(\nu_0, \nu_c, \bar{p}_c, \bar{N})$  imply that  $I[\nu_c, p_c, N, \bar{T}(p)]$  is smaller than  $\bar{I}(\nu_c)$  for  $p_c > \bar{p}_c$ . Since the values of  $R'(\nu_0, \nu_i, \bar{p}_c, \bar{N})$  are negative,  $T(p) < \bar{T}(p)$  for  $p_c > 0$ ; hence, the discrepancy between  $I[\nu_c, p_c, N, T(p)]$  and  $\bar{I}(\nu_c)$  will be even larger than that between  $I[\nu_c, p_c, N, \bar{T}(p)]$  and  $\bar{I}(\nu_c)$ .

An automatic process for adjusting cloud height will depend on the discrepancies between  $I[\nu_c, p_c, N, T(p)]$  and  $\bar{I}(\nu_c)$ . From Eq. (11), negative values of  $R(\nu_0, \nu_c, \bar{p}_c)$  and  $p_c > \bar{p}_c$  imply that if the computed cloud height and cloud amount that satisfy the observed radiance for the channel  $\nu_0$  will

always result in an outgoing radiance that is too small for the channel  $\nu_c$ . For the case shown in Fig. 1a with positive values of  $R(\nu_0, \nu_i, \bar{p}_c)$  and negative values of  $R(\nu_0, \nu_c, \bar{p}_c)$ , if  $I[\nu_c, p_c, N, T(p)] < \bar{I}(\nu_c)$ , we conclude that  $p_c$  is too large (i.e., the cloud top is too low) and should be adjusted to a higher level.

The following steps describe a detailed algorithm for deriving temperature profiles in the presence of clouds:

1. Choose an initial temperature profile  $T^0(p)$ , an initial cloud height  $p_c^0$ , and an initial cloud amount  $N^0$ .
2. Calculate  $I^j(\nu_i)$  for all channels and compute the temperature profile  $T^{j+1}(p)$  as described in Section 2, where  $j$  is the number of iteration.
3. If the calculated surface air temperature  $T^{j+1}(p_s)$  is within  $1^\circ\text{C}$  of the earth's surface temperature  $T_s$ , go to step 5. Otherwise go to the next step.
4. Adjust cloud amount  $N^j$  by a small positive amount  $\Delta N$ . If  $T^{j+1}(p_s) > T_s$ ,  $N^j$  is replaced by  $N^j - \Delta N$ ; if  $T^{j+1}(p_s) < T_s$ ,  $N^j$  is replaced by  $N^j + \Delta N$ . Return to step 2.
5. Compute the value of  $I^{j+1}(\nu_c)$ . If  $|I^{j+1}(\nu_c) - \bar{I}(\nu_c)|$  is smaller than the noise level of the instrument, then  $T^{j+1}(p)$ ,  $p_c^j$  and  $N^j$  are the approximate solutions. Otherwise go to the next step.
6. If  $I^{j+1}(\nu_c) > \bar{I}(\nu_c)$ , then  $p_c^j$  is too small (i.e., the cloud top is too high), and it is adjusted by a small positive amount  $\Delta p$  as  $p_c^{j+1} = p_c^j + \Delta p$ . If  $I^{j+1}(\nu_c) < \bar{I}(\nu_c)$ , then the cloud height is adjusted as  $p_c^{j+1} = p_c^j - \Delta p$ . Return to step 2.

## 5. Numerical experiments

The profiles used for simulating the outgoing radiance were taken from mid-latitude radiosonde observations for the month of April with arbitrary cloud height and cloud amounts. The simulated satellite "observed" radiances were calculated from Eq. (1), including random instrument noise. Standard deviations of the random errors are listed in Table 1, except the noise level for the  $668.5\text{ cm}^{-1}$  channel is reduced to  $0.59\text{ erg cm}^{-2}\text{ s}^{-1}\text{ sr}^{-1}\text{ cm}$ . Temperature profiles were then computed from the procedures discussed in Section 2, and cloud heights were adjusted according to the algorithm described in Section 4. The first guess in deriving temperature profiles was taken from the April Standard Atmosphere for mid-latitude.

In this study, three numerical experiments are performed. From Table 1, it can be seen that there are three channels with peaks of the Planck-modified weighting function located at the surface. In the derivation of the temperature profiles only one of these three cloud channels, together with the other eight channels is used.

Fig. 3 shows rms temperature errors as a function of cloud height errors for two cloudy situations. The

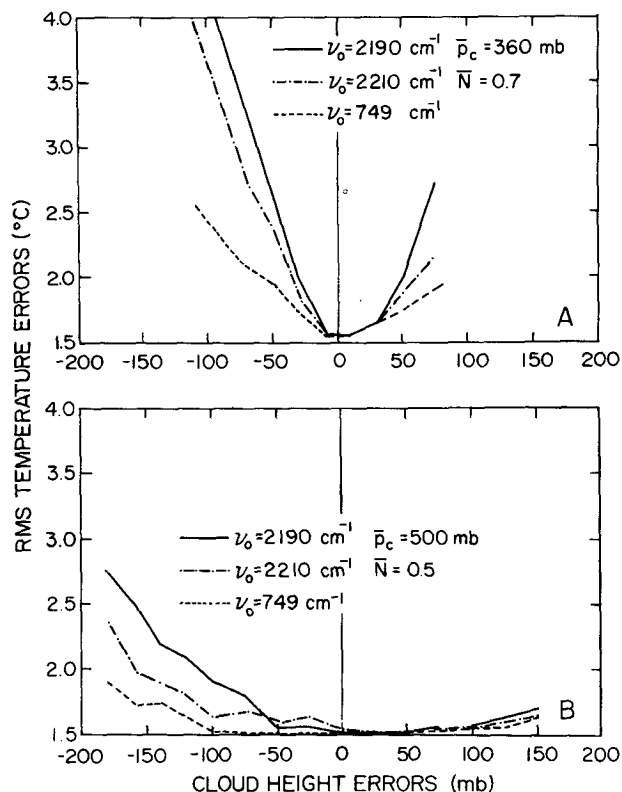


FIG. 3. Root mean square temperature errors as functions of cloud height errors for two cases. In the first case (Fig. 3a) where heavy cloud cover and high clouds are assumed, the sensitivity to cloud height errors is greatest when channel  $\nu_0 = 2190\text{ cm}^{-1}$  is used for cloud amount. In the second case (Fig. 3b) for medium cloud conditions, the temperature errors are less sensitive to cloud height errors. The channel with largest response in both cases is  $\nu_0 = 2190\text{ cm}^{-1}$ .

first case shown in Fig. 3a is for high clouds with heavy cloud cover (i.e.,  $\bar{p}_c = 360\text{ mb}$  and  $\bar{N} = 0.7$ ) and the second case shown in Fig. 3b is for lower clouds and medium cloud cover (i.e.,  $\bar{p}_c = 500\text{ mb}$  and  $\bar{N} = 0.5$ ). In both cases, the rms errors are almost  $1.6^\circ\text{C}$  when the prescribed cloud heights are close to the actual cloud heights. As the cloud height error increases, the rms error in the derived temperature profiles also increases; moreover, it increases faster for  $\nu_0 = 2190\text{ cm}^{-1}$  than for  $\nu_0 = 749$  and  $2210\text{ cm}^{-1}$ . It also can be seen in comparing Figs. 3a and 3b that the rms errors of the derived temperature profiles are more sensitive to cloud height errors for high clouds with heavy cloud cover. For  $\nu_0 = 2190\text{ cm}^{-1}$ , Fig. 3b shows the rms error increases only slightly from  $1.5$  to  $1.8^\circ\text{C}$  as  $p_c$  changes from  $500$  to  $400\text{ mb}$ , but in Fig. 3a it increases rapidly from  $1.5$  to  $3.9^\circ\text{C}$  as  $p_c$  changes from  $360$  to  $260\text{ mb}$ . These results are in agreement with the values of  $R'(\nu_0, \nu_i, \bar{p}_c, \bar{N})$  shown in Fig. 2.

Figs. 4 and 5 show the differences between the derived and the exact temperatures for two cloud

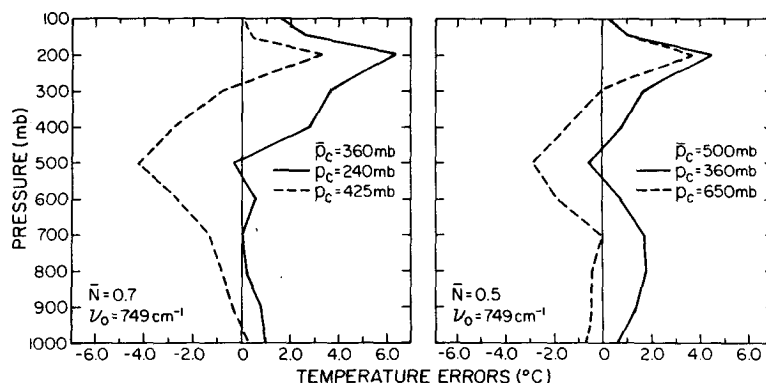


FIG. 4. Temperature errors as a function of pressure for  $\nu_0 = 749 \text{ cm}^{-1}$ .  $p_c$  is the prescribed cloud height, and  $\bar{p}_c$  and  $\bar{N}$  are the exact cloud heights and amounts. The solid line indicates that overestimating the cloud height produces warmer profiles than the exact temperature profiles and the dashed lines show that underestimating cloud height produces colder profiles.

conditions for  $\nu_0 = 749$  and  $2190 \text{ cm}^{-1}$ . In both cases it is seen that the derived temperatures are consistently larger than the exact ones if  $p_c < \bar{p}_c$  and are smaller than the exact ones if  $p_c > \bar{p}_c$ . The differences,  $T(p) - \bar{T}(p)$ , are largest for the case with  $\nu_0 = 2190 \text{ cm}^{-1}$ ,  $\bar{p}_c = 360 \text{ mb}$  and  $\bar{N} = 0.7$ . These results are as expected from the signs and magnitudes of  $R'(\nu_0, \nu_i, \bar{p}_c, \bar{N})$  shown previously in Fig. 2.

The radiances  $I(\nu_i)$  computed for a prescribed cloud height from which the derived temperature profile and cloud amount were obtained agrees with the measured radiances  $\bar{I}(\nu_i)$  by definition of solution. When the derived temperature profile and cloud amount are substituted in the cloud-sensing channel  $\nu_c$ , the computed radiance  $I(\nu_c)$  will, in general, not agree with the "observed" radiance  $\bar{I}(\nu_c)$ .

Fig. 6 shows the percent of radiance error,  $[I(\nu_c) - \bar{I}(\nu_c)]/\bar{I}(\nu_c) \times 100$ , in the cloud-sensing channel as a function of cloud height errors for two cases. In both cases, the cloud-sensing channel is  $\nu_c = 2190 \text{ cm}^{-1}$  and the channel for cloud amount is  $749 \text{ cm}^{-1}$ . Fig. 6a is the case with high clouds and heavy cloud cover, i.e.,  $\bar{p}_c = 360 \text{ mb}$  and  $\bar{N} = 0.7$  and Fig. 6b is the case

with lower clouds and less cloud cover, i.e.,  $\bar{p}_c = 500 \text{ mb}$  and  $\bar{N} = 0.5$ . Since the values of  $R(\nu_0, \nu_c, \bar{p}_c)$  shown in Fig. 1 are negative, values of  $I(\nu_c) - \bar{I}(\nu_c)$  are negative for  $p_c > \bar{p}_c$  and positive for  $p_c < \bar{p}_c$ . Although the rms errors of the derived temperature profiles are less sensitive to the cloud height errors for low clouds and small cloud amount, cloud height is more difficult to adjust. This is seen in Fig. 6b where the change of the percent of radiance error in the cloud-sensing channel is about 5.4% per 100 mb while that in Fig. 6a is about 20% per 100 mb. For the same errors in cloud heights, the discrepancy between  $I(\nu_c)$  and  $\bar{I}(\nu_c)$  for the latter case is about four times larger than that for the former case and, accordingly, the cloud height is easier to adjust for the latter case. In both cases, however, the use of the  $2190 \text{ cm}^{-1}$  channel for adjusting the cloud heights is very efficient.

Figs. 6a and 6b also yields a cloud amount determined from the cloud height algorithm which searches for the value of  $p_c$  which gives a minimum radiance error compared with the "observed" radiance in the cloud-sensing channel  $\nu_c$ . In both cases the correct cloud amounts were obtained.

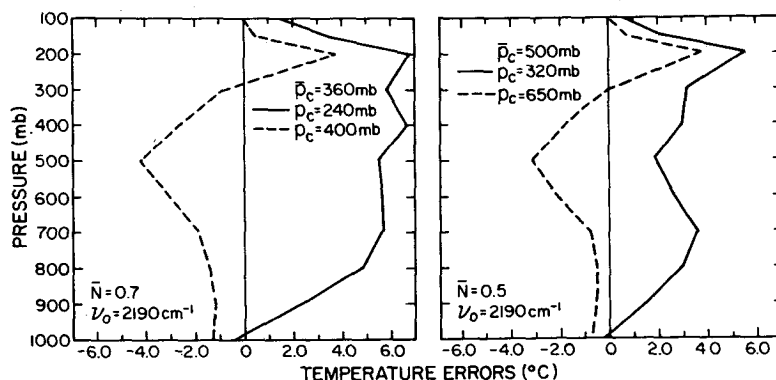


FIG. 5. As in Fig. 4 except for  $\nu_0 = 2190 \text{ cm}^{-1}$ .

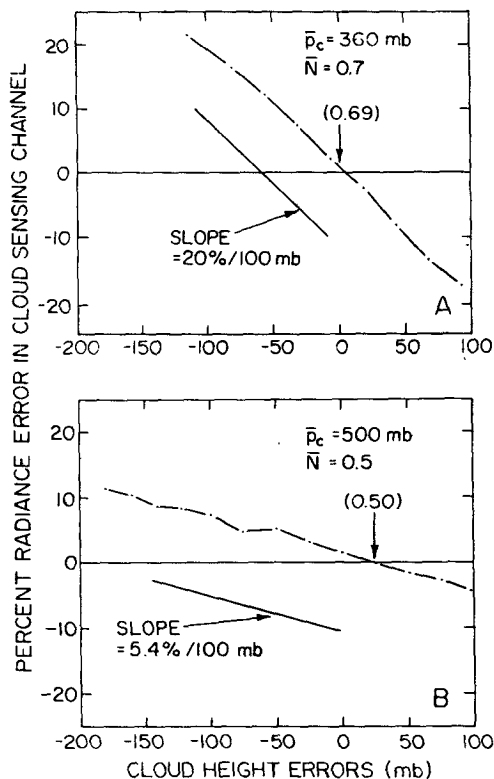


FIG. 6. Percentage of errors between the computed and measured radiances in the cloud-sensing channel,  $\nu_c = 2190 \text{ cm}^{-1}$ . The sign of these errors indicate the direction for adjusting the cloud height. A positive error indicates cloud height is overestimated and should be lowered. It is seen in Fig. 6a that errors are more sensitive under heavy cloud cover and high clouds. The values in parentheses are the derived cloud amounts.

## 6. Conclusions

If maximum performance is to be obtained from future multispectral range sounders, then careful consideration of cloud effects on the choice of channels becomes a principal factor. The response function  $R'(\nu_0, \nu_i, \bar{p}_c, \bar{N})$  provides a useful measure for determining the effects of cloud height errors on the

derived temperature profiles. The magnitudes and signs of the errors expected in the temperature profiles can be estimated from this function. If the magnitudes of the response function are large, then the errors induced in the derived temperature profile will also be large. Moreover, if the values of the response function are positive and the cloud height is overestimated (i.e.,  $p_c < \bar{p}_c$ ), then the derived temperatures will tend to be warmer than the actual temperatures.

In selecting channels, simulation studies for the proposed instrument should be carried out to determine the set of channels in the spectral ranges chosen that minimize the values of the response function to cloud effects. Furthermore, the values of the response function will indicate which channels would be best for cloud filtering. The governing principle in selecting channels to determine cloud heights is to maximize the spreads between the values of  $R'(\nu_0, \nu_i, \bar{p}_c, \bar{N})$  and  $R'(\nu_0, \nu_c, \bar{p}_c, \bar{N})$  in order to be more sensitive to cloud height errors. A large discrepancy between the computed and measured radiances in the cloud sensing channel makes it easier to adjust the cloud heights. Results show that the best choice for this purpose is usually the most transparent channel in the  $4.3 \mu\text{m}$  range.

On the other hand, somewhat different considerations should be given to determining cloud amounts. Since surface temperatures are available from other instruments, a relatively transparent channel with its Planck-modified weighting function located at the surface is not as helpful as would be a less transparent channel with its peak located at, say, 800 mb. In this case, the magnitude of the response function  $R'(\nu_0, \nu_i, \bar{p}_c, \bar{N})$  will be smaller, and the spread between  $R'(\nu_0, \nu_i, \bar{p}_c, \bar{N})$  and  $R'(\nu_0, \nu_c, \bar{p}_c, \bar{N})$  will be even larger.

## REFERENCES

- Chahine, M. T. 1974: Remote sounding of cloudy atmospheres. I. The single cloud layer. *J. Atmos. Sci.*, **31**, 233-243.
- Jastrow, R., and M. Halem, 1973: Accuracy and coverage of temperature data derived from the IR radiometer on the NOAA 2 satellite. *J. Atmos. Sci.*, **30**, 958-964.